

A Combined Experimental-Theoretical Study of the LigW-Catalyzed Decarboxylation of 5-Carboxyvanillate in the Metabolic Pathway for Lignin Degradation

Xiang Sheng,^{†,||} Wen Zhu,^{‡,||} Jamison Huddleston,[§] Dao Fen Xiang,[§] Frank M. Raushel,^{*,§} Nigel G. J. Richards,^{*,‡} and Fahmi Himo^{*,†}

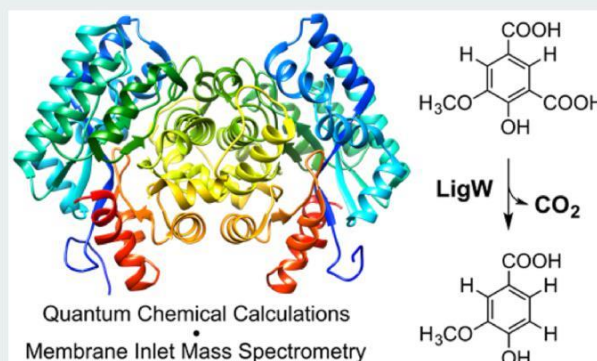
[†]Department of Organic Chemistry, Arrhenius Laboratory, Stockholm University, SE-106 91 Stockholm, Sweden

[‡]School of Chemistry, Cardiff University, Park Place, Cardiff CF10 3AT, U.K.

[§]Department of Chemistry, Texas A&M University, College Station, Texas 77843, United States

ABSTRACT: Although it is a member of the amidohydrolase superfamily, LigW catalyzes the nonoxidative decarboxylation of 5-carboxyvanillate to form vanillate in the metabolic pathway for bacterial lignin degradation. We now show that membrane inlet mass spectrometry (MIMS) can be used to measure transient CO₂ concentrations in real time, thereby permitting us to establish that C–C bond cleavage proceeds to give CO₂ rather than HCO₃[−] as the initial product in the LigW-catalyzed reaction. Thus, incubation of LigW at pH 7.0 with the substrate 5-carboxyvanillate results in an initial burst of CO₂ formation that gradually decreases to an equilibrium value as CO₂ is nonenzymatically hydrated to HCO₃[−]. The burst of CO₂ is completely eliminated with the simultaneous addition of substrate and excess carbonic anhydrase to the enzyme, demonstrating that CO₂ is the initial reaction product. This finding is fully consistent with the results of density functional theory calculations, which also provide support for a mechanism in which protonation of the C5 carbon takes place prior to C–C bond cleavage. The calculated barrier of 16.8 kcal/mol for the rate-limiting step, the formation of the C5-protonated intermediate, compares well with the observed *k*_{cat} value of 27 s^{−1} for *Sphingomonas paucimobilis* LigW, which corresponds to an energy barrier of ~16 kcal/mol. The MIMS-based strategy is superior to alternate methods of establishing whether CO₂ or HCO₃[−] is the initial reaction product, such as the use of pH-dependent dyes to monitor very small changes in solution pH. Moreover, the MIMS-based assay is generally applicable to studies of all enzymes that produce and/or consume small-molecule, neutral gases.

KEYWORDS: decarboxylase, membrane inlet mass spectrometry, reaction mechanism, cluster approach, density functional theory, quantum chemistry



INTRODUCTION

5-Carboxyvanillate decarboxylase (LigW) catalyzes the formation of vanillate (3-methoxy-4-hydroxybenzoate) via the nonoxidative decarboxylation reaction shown in Scheme 1a. LigW is an integral component within the biochemical degradation pathway of lignin from plant biomass by bacteria. Although LigW is a member of the amidohydrolase superfamily (AHS), this enzyme is located within a subset from cog2159 that catalyzes decarboxylation reactions rather than the much more common hydrolysis of carboxylate and phosphate esters performed by other AHS members.¹ Recently, we interrogated the chemical reaction mechanism of LigW using the enzymes from *Sphingomonas paucimobilis* and *Novosphingobium aromaticivorans* by high-resolution X-ray crystallography, mutation of active site residues, substrate–activity relationships, and product isotope effects.² These studies led to the conclusion that LigW catalyzes the decarboxylation of 5-carboxyvanillate

(5-CV) via a reaction intermediate formed by protonation of the substrate at C5 prior to carbon–carbon bond cleavage, as shown in Scheme 1b.

Experimental support for the existence of the C5-protonated intermediate was provided by the 1.07 Å resolution X-ray structure of the tight-binding substrate analogue 5-nitrovanillate (5-NV) in the active site of LigW (Figure 1). In this very high resolution X-ray crystal structure (PDB ID: 4QRN) the nitro substituent of the inhibitor is clearly bent out of the plane of the phenyl ring by approximately 23° in a manner that is consistent with an enzyme-induced conformational change that facilitates protonation of the substrate at C5 by Asp314.² The product isotope effect of 4.6, determined in an equal mixture of

Scheme 1. (a) Reaction Catalyzed by LigW, (b) Proposed Reaction Mechanism, and (c, d) Alternative Pathways Resulting in Bicarbonate as the Initial Reaction Product

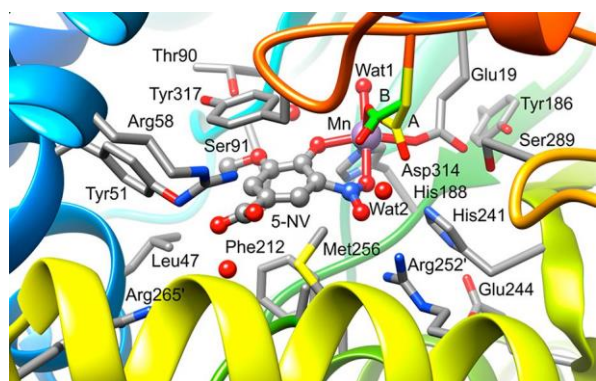
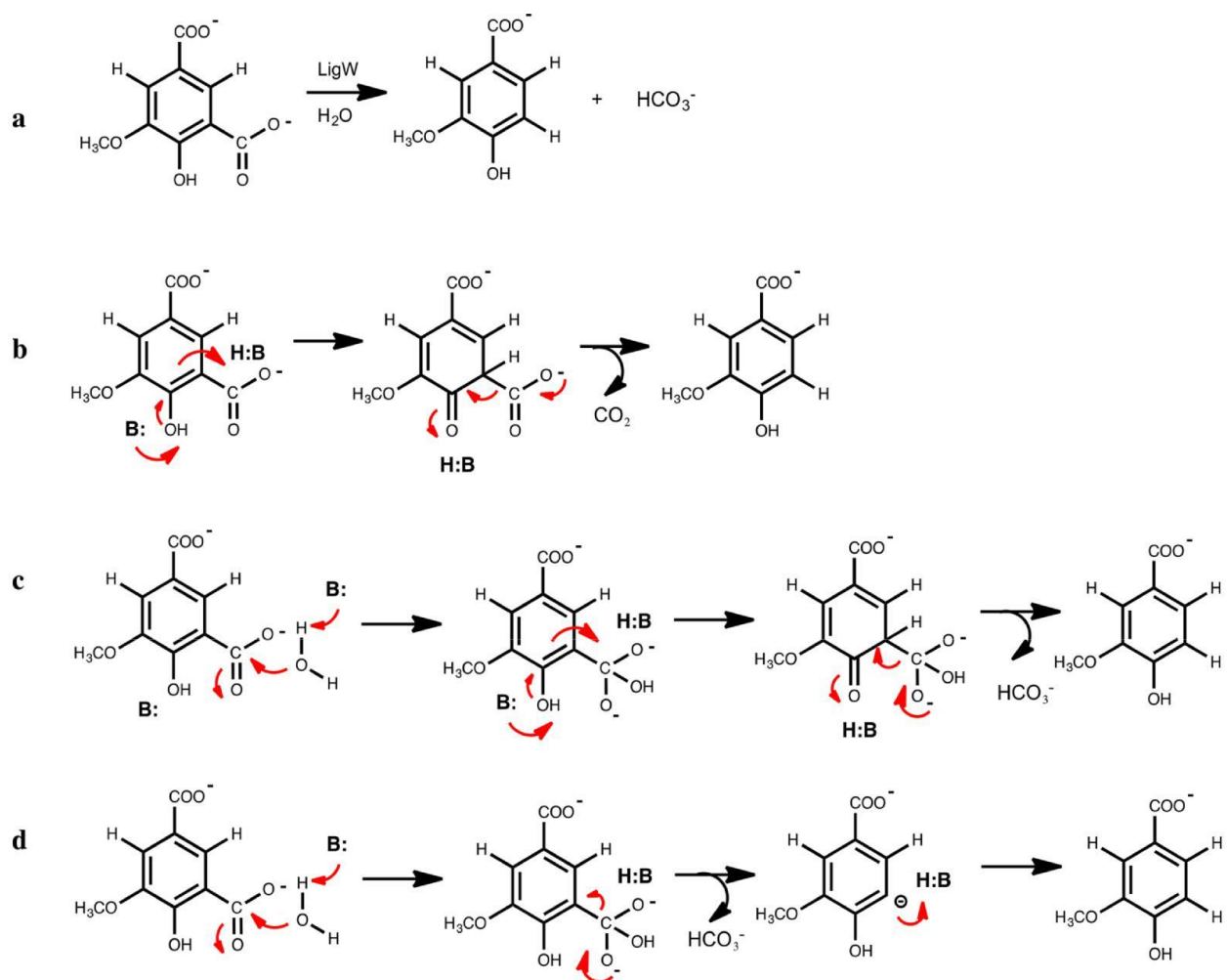


Figure 1. Crystal structure of the LigW active site in complex with the 5-NV inhibitor (PDB ID: 4QRN). The two conformations of Asp314 are indicated as A and B.

H₂O and D₂O, supports C5 protonation of the substrate prior to, rather than after, carbon-carbon bond cleavage.

This prior investigation, however, did not address the question of whether the initial decarboxylation product is carbon dioxide or bicarbonate. It has been argued previously that HCO₃⁻ can be mechanistically preferred as the initial reaction product relative to CO₂ in many enzyme-catalyzed decarboxylation reactions.³⁻⁵ This conclusion is based, in part,

on the high chemical reactivity of CO₂, which can significantly diminish the partitioning of the various enzyme-ligand complexes toward net product formation by increasing the rate of internal return of these complexes back to substrate, relative to the rate at which products are released from the active site. Calculations on model systems provide some support for the view that the barrier to internal return is very low when carbon dioxide is the initial product.⁶ It is therefore of interest to note that, in the high-resolution X-ray structure of LigW bound to 5-NV, water molecules are in a position to participate in an enzyme-catalyzed hydration of the C5-carboxylate in the substrate. Irrespective of whether the hydration reaction takes place before or after proton transfer to C5, alternative mechanisms can be written for the LigW-catalyzed reaction that would ultimately result in HCO₃⁻ being the initial reaction product, rather than CO₂, as shown in Scheme 1c,d.²

Here we utilize an integrated experimental and computational strategy to probe the catalytic mechanism and the structure of reaction intermediates in the conversion of 5-carboxyvanillate to vanillate in the reaction catalyzed by LigW. First, membrane inlet mass spectrometry (MIMS)⁷ measurements of the initial rate of CO₂ production at pH 7.0, in combination with kinetic simulations, provide strong experimental evidence for CO₂ being the actual product of the LigW-

catalyzed reaction. Second, complementary theoretical calculations on the reaction mechanism, performed with density functional theory, are fully consistent with the formation of CO₂ as the initial product of C–C bond cleavage from a C5-protonated reaction intermediate. These findings not only help to more firmly establish the catalytic reaction mechanism employed by LigW but also demonstrate the power of MIMS to discriminate between CO₂ and HCO₃[−] production in enzyme-catalyzed reactions.

EXPERIMENTAL SECTION

Experimental Methods. LigW from *N. aromaticivorans* was prepared as previously described.² Membrane inlet mass spectrometry (HDR-20) was used to monitor the rate of CO₂ formation of the LigW-catalyzed decarboxylation of 5-CV. A solution of buffer (a mixture of 100 mM HEPES and 100 mM MES titrated to pH 7.0) and variable amounts of 5-CV (0–800 μM) were placed in the reaction chamber (2 mL total volume) and equilibrated for 2 min at 25 °C. Reactions were initiated by the addition of LigW (0–1.6 μM), and CO₂ production was determined in real time by monitoring the ion current at 44 m/z. The ion current signal was converted to the concentration of CO₂ using a standard curve, which was determined under the same buffer conditions as the LigW-catalyzed reactions by adding known amounts of K₂CO₃ to a 2.0 mL reaction mixture in the absence of enzyme. The CO₂ concentration was then calculated using the apparent dissociation constant for H₂CO₃ (pK_a = 6.35) under the assumption that all of the H₂CO₃ would dissociate into CO₂. For some experiments carbonic anhydrase (0–500 μg) was added prior to the addition of LigW in order to more rapidly equilibrate the interconversion between carbon dioxide and bicarbonate. The kinetics simulations were conducted using Kintek Global Kinetic Explorer student version 6.0.⁸

Computational Methods. All calculations presented here were performed using the B3LYP hybrid density functional method,^{9,10} as implemented in the Gaussian 09 program.¹¹ Geometry optimization was carried out with the 6-31G(d,p) basis set for C, N, O, and H and LANL2DZ¹² pseudopotential for Mn, and dispersion corrections were included using the DFT-D3(BJ) method.^{13,14} To obtain more accurate energies, single-point calculations on the optimized structures were performed with LANL2DZ for Mn and the larger basis set 6-311+G(2d,2p) for the other atoms. The SMD solvation model was used to model the effects of the rest of the enzyme that was not included in the model.¹⁵ Single-point energies, at the same level of theory as the geometry optimization, were calculated with the value of the dielectric constant $\epsilon = 4$. Frequency calculations were performed to obtain zero-point energies (ZPE) at the same level of theory. Energies reported herein are thus those for the large basis set (which include dispersion) corrected for ZPE and solvation effects. During the geometry optimizations, a number of atoms were fixed at their crystallographic positions to prevent unrealistic residue movements. As in previous studies on similar enzymatic reactions,^{16–18} the entropy gain from releasing a small gas molecule was estimated to be the translational entropy of the free molecule. This yields a calculated entropy for CO₂ release of 11.1 kcal/mol at room temperature, which is added to the energy of the CO₂ formation step. Transition states were fully optimized on the basis of initial manual scans of appropriate coordinates. The nature of the connecting stationary points was confirmed by slightly disturbing the structures of transition

states manually and reoptimizing in the forward and backward directions.

RESULTS AND DISCUSSION

Measuring the Rate of CO₂ Production using MIMS.

Membrane inlet mass spectrometry (MIMS) permits the real-time detection of small, neutral gas concentrations in solution⁷ and has been used to study the steady-state kinetics of a

number of enzymes, including carbonic anhydrase

^{19,20} and

oxalate^{21,22} decarboxylase.

In the MIMS-based approach, a probe covered by a semipermeable membrane is present in the reaction mixture during the enzyme-catalyzed transformation. As a result, neutral, low-molecular-weight volatile organic compounds and gas molecules present in solution diffuse through the membrane, driven by a pressure differential, and then travel into a standard mass spectrometer to generate an ion current that is proportional to their concentration. The use of substrates that are labeled with stable isotopes ensures that gases produced by the enzyme can be differentiated from those already present in solution. It is also important to note that ion currents for multiple gases can be measured simultaneously in real time, enhancing the utility of MIMS in studies of enzyme catalysis relative to other methods, such as the Clark electrode.

In this study, MIMS measurements were used to determine the rate of CO₂ production in real time as a function of LigW concentration. An apparent burst of CO₂ formation was observed immediately after mixing LigW (1.5 μM) with 5-carboxyvanillate (500 μM) at pH 7.0, with the CO₂ concentration reaching a maximum of approximately 250 μM at ~30 s before gradually diminishing to an equilibrium value of ~125 μM after 120 s (Figure 2a). This time course is consistent with a rapid initial enzymatic formation of CO₂ that is subsequently converted nonenzymatically to an equilibrium

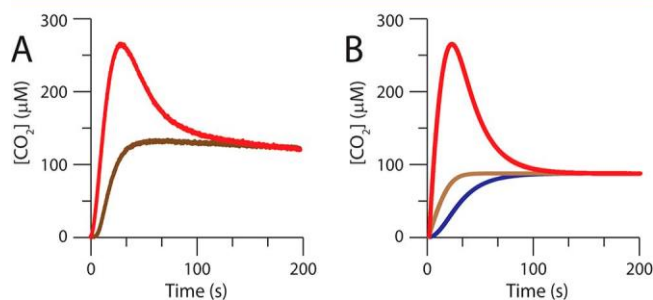


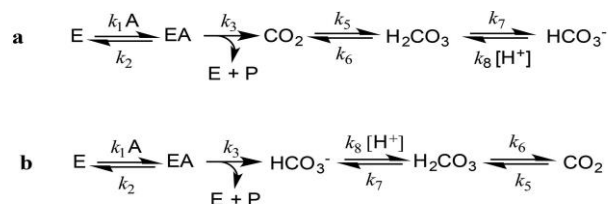
Figure 2. Experimental and simulated time courses for the production of CO₂ during the LigW catalyzed decarboxylation of 5-carboxyvanillate: (A) experimental time courses for the formation of CO₂ when 1.5 μM LigW was added to a solution of 500 μM 5-carboxyvanillate at pH 7.0 in the presence (tan) or absence (red) of 1.0 μg of carbonic anhydrase; (B) simulated time courses for the formation of CO₂ at pH 7.0 when it is assumed that either CO₂ (red) or HCO₃[−] (blue) is the initial reaction product during the LigW-catalyzed decarboxylation of 5-carboxyvanillate. The time course depicted in tan is for a model where CO₂ is the initial reaction product and excess carbonic anhydrase has been added to catalyze the rapid interconversion of CO₂ to HCO₃[−]. The simulations were conducted using the kinetic models depicted in Scheme 2a (CO₂ as initial product) and Scheme 2b

(HCO₃[−] as the initial product) where [E] = 1.5 μM, [A] = 500 μM, [H⁺] = 0.10 μM, $k_1 = 10 \mu\text{M}^{-1} \text{s}^{-1}$, $k_2 = 2.5 \times 10^3 \text{s}^{-1}$, $k_3 = 27 \text{s}^{-1}$, $k_5 = 0.04 \text{s}^{-1}$, $k_6 = 28 \text{s}^{-1}$, $k_7 = 1.5 \times 10^6 \text{s}^{-1}$, and $k_8 = 4.7 \times 10^4 \text{mM}^{-1} \text{s}^{-1}$. In the presence of excess carbonic anhydrase, the values of k_5 and k_6 were estimated as being greater than 1.4 and 1000 s^{-1} , respectively.

mixture of CO_2 and HCO_3^- at a slower rate. The magnitude of the burst of CO_2 formation was dependent on the concentration of LigW and was eliminated when carbonic anhydrase (1.0 μg) was also present in the reaction mixture (Figure 2a and the Supporting Information). This finding is consistent with the idea that CO_2 is the initial product of the LigW-catalyzed reaction because carbonic anhydrase increases the rate of the equilibration of CO_2 and HCO_3^- . Similarly, varying the amount of carbonic anhydrase present in the reaction mixture at fixed substrate modulated the magnitude of the burst phase at pH 7.0 (see the Supporting Information). In addition to providing unambiguous information on the nature of the initial product of the LigW-catalyzed reaction, these experiments illustrate the technical simplicity and rapid nature of the MIMS-based assay that might be contrasted with other approaches, such as that used to demonstrate that CO_2 is the true reaction product of OMP decarboxylase.²³

Numerical Simulations of LigW-Catalyzed Decarboxylation. In order to validate our interpretation of the MIMS observations, time courses for decarboxylation of 5-CV by LigW were simulated numerically assuming the initial formation of either CO_2 or HCO_3^- . In a minimal kinetic model for the former reaction, substrate (A) binds to enzyme (E) to form a Michaelis complex (EA), which subsequently undergoes irreversible decarboxylation (k_3) to form product (P) and CO_2 (Scheme 2a). CO_2 is then converted non-

Scheme 2. Alternative Kinetic Models for the LigW-Catalyzed Reaction



enzymatically to HCO_3^- via the intermediacy of H_2CO_3 . Alternatively, we investigated the behavior of a kinetic model in which the initial reaction product was assumed to be HCO_3^- , which also undergoes a nonenzymatic equilibration to CO_2 (Scheme 2b). The rate for the first half of this transformation clearly depends on the amount of LigW, while that of the second half is modulated by the presence (or absence) of carbonic anhydrase in the reaction mixture. As a result, a burst of CO_2 is expected for the mechanism depicted in Scheme 2a whenever the rate of CO_2 formation exceeds that of its nonenzymatic conversion to HCO_3^- , with a lag in CO_2 formation being predicted when HCO_3^- is the initial reaction product. This is evident from the simulated time courses at pH 7.0 for the initial formation of either CO_2 or HCO_3^- using appropriate values for k_1 through k_8 (Figure 2b). Thus, the dissociation constant for the Michaelis complex EA (k_2/k_1) was assumed to be equal to the Michaelis constant for 5-CV with LigW (250 μM)² with k_2 being $\geq 2.5 \times 10^3 \text{ s}^{-1}$. The value of k_3 was set to k_{cat} for the decarboxylation of 5-CV,² and rate constants for the hydration of CO_2 (k_5) and dehydration of carbonic acid (k_6) were based on literature values.²⁴ The rate constant for protonation of HCO_3^- (k_8) has been reported by Eigen,²⁵ and the value of k_7 was obtained from the pK_a of carbonic acid (3.6). When the simulations were used to predict the time courses for CO_2 formation in the presence of excess

carbonic anhydrase, the values of k_5 and k_6 were estimated as being greater than 1.4 and 1000 s^{-1} , respectively. The experimental time course at pH 7.0 is clearly only consistent with the simulations in which formation of CO_2 , and not HCO_3^- , is the initial reaction product in the LigW-catalyzed decarboxylation reaction (Figure 2).

Density Functional Calculations. Density functional theory (DFT) calculations employing the cluster approach, which has been used extensively to study a wide variety of enzymatic reactions,^{26–30} were also used to examine the feasibility of the catalytic mechanism proposed previously for the LigW-catalyzed reaction. A model of the LigW active site was constructed from the high-resolution crystal structure of the enzyme in complex with the inhibitor 5-NV (PDB ID: 4QRN).² The model consists of the Mn^{2+} cation along with its ligands (Glu19, His188, Asp314, Wat1, and 5-NV/5-CV), nine other crystallographic water molecules, residues that potentially form hydrogen bonds with 5-NV/5-CV directly or via water molecules (Tyr51, Arg58, Thr90, Gly207, Ala208, His241, Arg252', and Arg265'), and residues that are π -stacked to the aromatic ring of the substrate (Phe212 and Tyr317). In addition, other residues that contribute to the active site pocket were included (Leu47, Ser91, Tyr186, Ile209, Val239, Gly240, Glu244, and Ser289). Amino acids were truncated as shown in Figure 3, and hydrogen atoms were added manually. In order to avoid unrealistic movements of the groups during the geometry optimizations, certain atoms were kept fixed to their crystallographic positions, as indicated in the figure. The hydroxyl group at C4 of 5-NV/5-CV is assumed to lose its proton upon binding to the Mn^{2+} cation in the active site. The model consists of 308 atoms and has a total charge of +2 or +1 for that with 5-NV (Figure 3a) or 5-CV (Figure 3b), respectively.

The optimized geometry of the enzyme-inhibitor structure (Figure 3a) resembles the crystal structure (Figure 1), with very similar metal-ligand distances and other geometric parameters. As indicated in Figure 1, two conformers were proposed for the Asp314 residue in the crystal structure (called A and B conformers). The side chain of Asp314 shown in Figure 3 is in a position similar to that of the A conformer. We also optimized a different structure of the enzyme-inhibitor complex, in which the carboxyl group of Asp314 points toward C5 of the substrate, corresponding to the B conformer (see the Supporting Information for the geometry). The energy difference between the two structures is 2 kcal/mol in favor of conformer A, which is in line with the measured occupancy in the X-ray structure (ca. 0.70:0.30). In the case of the enzyme-substrate complex, the energy difference between the two conformers is only 0.4 kcal/mol, in favor of conformer A.

It is interesting to note that the calculations reproduce very well the distortion of the inhibitor geometry observed in the crystal structure. The bending of the nitro substituent relative to the phenyl ring is calculated to be $\sim 16^\circ$ (22° in the B conformer; see the Supporting Information) in comparison with $\sim 23^\circ$ in the crystal structure. Very interestingly, the substrate was also bent when bound in the active site. The angle between the carboxylate and the phenyl ring is calculated to be $\sim 17^\circ$ (Figure 3b).

Starting from the enzyme-substrate complex (Figure 3b), we examined different mechanistic scenarios for the LigW reaction. The reaction pathway with the most plausible energies is shown in Figure 4 along with the energy profile, and optimized structures of transition states and intermediates are given in Figure 5. The two-step mechanism starts with a proton

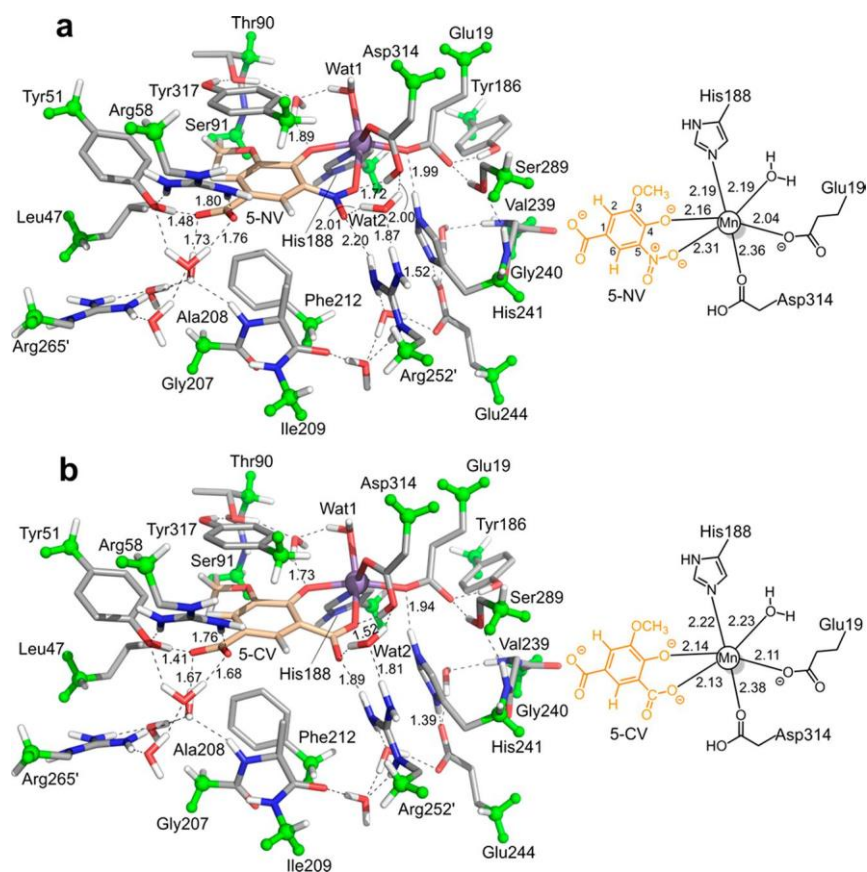


Figure 3. Optimized structures of the active site model with (a) the 5-NV inhibitor and (b) the 5-CV substrate bound. For clarity, only polar hydrogen atoms and hydrogens on the substrate and truncated bonds are shown. Atoms fixed during geometry optimization are shown in green.

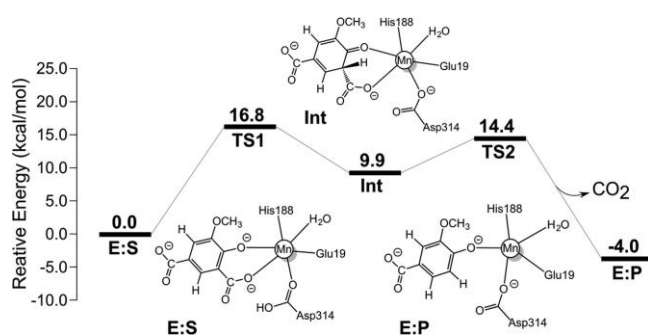


Figure 4. Calculated energy profile for the mechanism obtained on the basis of the DFT study.

transfer from Asp314 to the C5 carbon of 5-CV. The barrier for this step is calculated to be 16.8 kcal/mol, and the resulting intermediate (Int) is 9.9 kcal/mol higher than the E:S complex. At the optimized transition state (TS1) for this step, the distances of the forming C-H and breaking O-H bonds are 1.36 and 1.33 Å, respectively. In comparison to the E:S complex, the coordination bond of Asp314 is shortened while the two coordination bonds of the substrate are elongated. His241 forms a hydrogen bond to the Mn-coordinated carboxylate group of the substrate at TS1 and changes to form a hydrogen bond with the deprotonated Asp314 in Int.

C-C bond cleavage then takes place, forming the vanillate product and leading to the release of CO₂. The barrier for this step is 4.5 kcal/mol relative to Int, i.e. 14.4 kcal/mol relative to E:S, and the resulting enzyme-product complex (E:P) is 13.9

kcal/mol lower than Int, i.e. -4.0 kcal/mol relative to E:S, including the entropy contribution from the release of CO₂. At the transition state of this step (TS2), the length of the breaking C-C bond is 1.99 Å. In the E:P structure, the water molecule Wat2 occupies the position where the carboxylate group of the substrate used to be. However, Wat2 is not coordinated to the Mn²⁺ cation, and the Mn²⁺ cation is therefore five-coordinated.³¹

The obtained barrier of 16.8 kcal/mol compares very well with the measured k_{cat} value of 27 s^{-1} ,² which corresponds to a rate-limiting barrier of ~16 kcal/mol according to classical transition state theory. The calculations also reproduce the measured kinetic isotope effect very well. By substituting the proton at Asp314 for a deuterium and recalculating the zero-point energy difference between the E:S complex and the rate-limiting TS1, we obtain a difference of 0.85 kcal/mol. This corresponds to a KIE of 4.2, which is in good agreement with the measured value of 4.6,² thus providing further support for the proposed mechanism.

In the structures of all stationary points, the side chain of Tyr317 forms a π - π interaction with the aromatic ring of the substrate. To evaluate the importance of this interaction, we designed a model in which Tyr317 was removed (effectively corresponding to a Tyr317Ala mutant). The rate-limiting barrier for this model was calculated to be 20.2 kcal/mol, which is 3.6 kcal/mol higher than the wild-type model (see the Supporting Information for the optimized structures and the calculated energy profile), showing that this residue is indeed important for catalysis. These results are consistent with the experimental mutation performed on the equivalent Tyr299

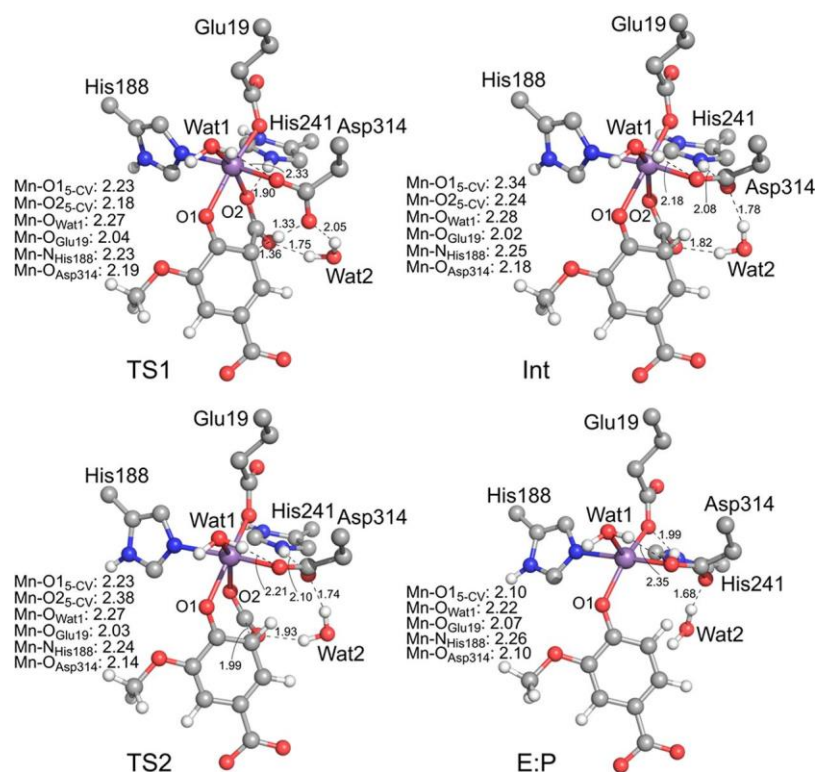


Figure 5. Optimized structures of the stationary points along the proposed reaction pathway. For clarity, only a small part of the model is shown here.

residue of LigW from *Sphingomonas paucimobilis*.² Namely, replacement of this residue by alanine reduced the activity of the enzyme by 4 orders of magnitude.

Very importantly, using the active site model of Figure 3b, we also investigated the possibility of bicarbonate as the initial product of the reaction rather than carbon dioxide (Scheme 1c,d). According to this hypothesis, a water molecule could add to the carboxylate group of the substrate either before or after the proton transfer from Asp314 to the C5 carbon of 5-CV. We have optimized structures of the intermediates that would result from these additions: i.e., with a hydrated carboxylate group (Figure 6). Both intermediates are calculated to have prohibitively high energies in comparison to the E:S complex,

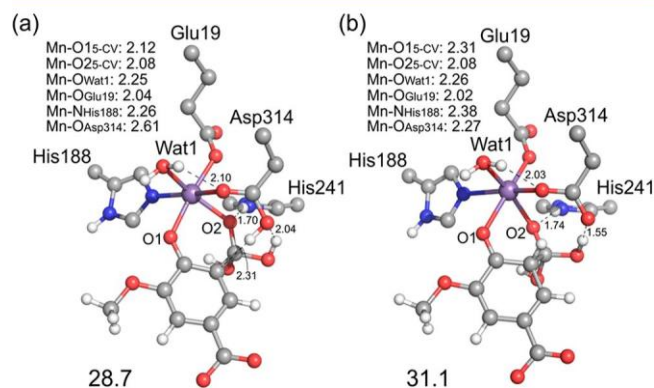


Figure 6. Optimized structures of the intermediates with a hydrated carboxylate group (a) before or (b) after the proton transfer process. The energies relative to the enzyme-substrate complex (Figure 3b) are given in kcal/mol. For clarity, only a part of the model is shown here.

ca. +30 kcal/mol. These energies are thus sufficient to rule out this mechanistic possibility. Similar conclusions were recently reached for another decarboxylase, phenolic acid decarboxylase.³² Namely, calculations on the reverse reaction, the carboxylation of hydroxystyrene, showed that the formation of the intermediate with a hydrated carboxylate group is not energetically feasible there either.

Another mechanistic alternative we examined in the current study is whether the decarboxylation can take place first, before the protonation of the substrate, leading to the generation of a carbanion intermediate. A similar mechanism has been suggested for the reaction of OMP decarboxylase.^{23,33,34} In the case of LigW, all attempts to optimize the geometry of the carbanion intermediate resulted in the structures of either the enzyme-substrate or enzyme-product complexes. An energy scan of the C-C bond starting from E:S shows that the energy increases monotonously to very high values, thus dismissing this mechanistic option (see the Supporting Information).

CONCLUSIONS

A straightforward MIMS-based assay has been used to demonstrate unequivocally that LigW catalyzes the decarboxylation of 5-carboxyvanillate to give CO₂ as the initial reaction product. This experimental observation is entirely consistent with DFT calculations that support a two-step catalytic mechanism which requires the formation of a C5-protonated intermediate prior to carbon-carbon bond cleavage and the formation of vanillate and carbon dioxide. Our results rule out alternate mechanisms in which HCO₃⁻ is the initial product of carbon-carbon bond cleavage. Moreover, this study shows the ability of MIMS-based assays to discriminate between CO₂ and HCO₃⁻ as the initial reaction product in enzyme-catalyzed decarboxylation reactions. Given the technical simplicity of

MIMS measurements, this methodology remains surprisingly underutilized in mechanistic enzymology in general, and specifically in studies of other decarboxylases.

ASSOCIATED CONTENT

Experimental time courses for the CO₂ production with different concentrations of LigW or carbonic anhydrase, optimized enzyme–inhibitor complex with Asp314 in B conformer, additional results concerning the Tyr317Ala mutant reaction, energy scan for the decarboxylation-first mechanism, and Cartesian coordinates of optimized structures

AUTHOR INFORMATION

Corresponding Authors

*E-mail for F.M.R.: raushel@tamu.edu.

*E-mail for N.G.J.R.: RichardsN14@cardiff.ac.uk.

*E-mail for F.H.: fahmi.himo@su.se.

ORCID

Xiang Sheng: 0000-0002-6542-6649

Frank M. Raushel: 0000-0002-5918-3089

Nigel G. J. Richards: 0000-0002-0375-0881

Fahmi Himo: 0000-0002-1012-5611

Author Contributions

||X.S. and W.Z. contributed equally to this work.

Notes

The authors declare no competing financial interest.

ACKNOWLEDGMENTS

This work was supported in part by the Robert A. Welch Foundation (A-840 to F.M.R.). F.H. acknowledges financial support from the Swedish Research Council and the Knut and Alice Wallenberg Foundations. Support from Cardiff University (W.Z.) is gratefully acknowledged.

REFERENCES

- (1) Seibert, C. M.; Raushel, F. M. *Biochemistry* 2005, 44, 6383–6391.
- (2) Vladimirova, A.; Patskovsky, Y.; Fedorov, A. A.; Fedorov, E. V.; Bonnano, J. B.; Toro, R.; Hillerich, B.; Seidel, R.; Richards, N. G. J.; Almo, S. C.; Raushel, F. M. *J. Am. Chem. Soc.* 2016, 138, 826–836.
- (3) Kluger, R. *Acc. Chem. Res.* 2015, 48, 2843–2849.
- (4) Kluger, R.; Howe, G. W.; Mundle, S. O. *C. Adv. Phys. Org. Chem.* 2013, 47, 85–128.
- (5) Howe, G. W.; Bielecki, M.; Kluger, R. *J. Am. Chem. Soc.* 2012, 134, 20621–20623.
- (6) Howe, G. W.; Kluger, R. *J. Org. Chem.* 2014, 79, 10972–10980.
- (7) Moral, M. E. G.; Tu, C.; Richards, N. G. J.; Silverman, D. N. *Anal. Biochem.* 2011, 418, 73–77.
- (8) Johnson, K. A.; Simpson, Z. B.; Blom, T. *Anal. Biochem.* 2009, 387, 20–29.
- (9) Becke, A. D. *J. Chem. Phys.* 1993, 98, 5648–5652.
- (10) Lee, C.; Yang, W.; Parr, R. G. *Phys. Rev. B: Condens. Matter Mater. Phys.* 1988, 37, 785–789.
- (11) Frisch, M. J.; Trucks, G. W.; Schlegel, H. B.; Scuseria, G. E.; Robb, M. A.; Cheeseman, J. R.; Scalmani, G.; Barone, V.; Mennucci, B.; Petersson, G. A.; Nakatsuji, H.; Caricato, M.; Li, X.; Hratchian, H. P.; Izmaylov, A. F.; Bloino, J.; Zheng, G.; Sonnenberg, J. L.; Hada, M.; Ehara, M.; Toyota, K.; Fukuda, R.; Hasegawa, J.; Ishida, M.; Nakajima, T.; Honda, Y.; Kitao, O.; Nakai, H.; Vreven, T.; Montgomery, J. A., Jr.; Peralta, J. E.; Ogliaro, F.; Bearpark, M.; Heyd, J. J.; Brothers, E.; Kudin,

- (12) Staroverov, V. N.; Keith, T.; Kobayashi, R.; Normand, J.; Raghavachari, K.; Rendell, A.; Burant, J. C.; Iyengar, S. S.; Tomasi, J.; Cossi, M.; Rega, N.; Millam, J. M.; Klene, M.; Knox, J. E.; Cross, J. B.; Bakken, V.; Adamo, C.; Jaramillo, J.; Gomperts, R.; Stratmann, R. E.; Yazyev, O.; Austin, A. J.; Cammi, R.; Pomelli, C.; Ochterski, J. W.; Martin, R. L.; Morokuma, K.; Zakrzewski, V. G.; Voth, G. A.; Salvador, P.; Dannenberg, J. J.; Dapprich, S.; Daniels, A. D.; Farkas, O.; Foresman, J. B.; Ortiz, J. V.; Cioslowski, J.; Fox, D. J. *Gaussian 09, Revision D.01*; Gaussian, Inc., Wallingford, CT, 2013.
- (13) Hay, P. J.; Wadt, W. R. *J. Chem. Phys.* 1985, 82, 270–283.
- (14) Grimme, S.; Antony, J.; Ehrlich, S.; Krieg, H. *J. Chem. Phys.* 2010, 132, 154104.
- (15) Grimme, S.; Ehrlich, S.; Goerigk, L. *J. Comput. Chem.* 2011, 32, 1456–1465.
- (16) Marenich, A. V.; Cramer, C. J.; Truhlar, D. G. *J. Phys. Chem. B* 2009, 113, 6378–6396.
- (17) Blomberg, M. R. A.; Siegbahn, P. E. M. *Biochemistry* 2012, 51, 5173–5186.
- (18) Lind, M. E. S.; Himo, F. *ACS Catal.* 2014, 4, 4153–4160.
- (19) Sheng, X.; Lind, M. E. S.; Himo, F. *FEBS J.* 2015, 282, 4703–4713.
- (20) Li, Y.; Tu, C. K.; Wang, H.; Silverman, D. N.; Frost, S. C. *J. Biol. Chem.* 2011, 286, 15789–15796.
- (21) McConnell, I. L.; Badger, M. R.; Wydrzynski, T.; Hillier, W. *Biochim. Biophys. Acta, Bioenerg.* 2007, 1767, 639–647.
- (22) Zhu, W.; Easton, L. M.; Reinhardt, L. A.; Tu, C. K.; Cohen, S. E.; Silverman, D. N.; Allen, K. N.; Richards, N. G. J. *Biochemistry* 2016, 55, 2163–2173.
- (23) Moral, M. E. G.; Tu, C. K.; Richards, N. G. J.; Silverman, D. N. *Chem. Commun.* 2011, 47, 3111–3113.
- (24) Porter, D. J. T.; Short, S. A. *Biochemistry* 2000, 39, 11788–11800.
- (25) Knoche, W. In *Biophysics and Physiology of Carbon Dioxide*; Bauer, C., Gros, G., Bartel, H., Eds.; Springer-Verlag: Berlin, Heidelberg, 1980; pp 3–11.
- (26) Eigen, M. *Angew. Chem.* 1963, 75, 489–508.
- (27) Siegbahn, P. E. M.; Himo, F. *JBIC, J. Biol. Inorg. Chem.* 2009, 14, 643–651.
- (28) Siegbahn, P. E. M.; Blomberg, M. R. A. *Chem. Rev.* 2010, 110, 7040–7061.
- (29) Siegbahn, P. E. M.; Himo, F. *Comput. Mol. Sci.* 2011, 1, 323–336.
- (30) Blomberg, M. R. A.; Borowski, T.; Himo, F.; Liao, R.-Z.; Siegbahn, P. E. M. *Chem. Rev.* 2014, 114, 3601–3658.
- (31) Himo, F. *J. Am. Chem. Soc.* 2017, 139, 6780–6786.
- (32) A concerted pathway involving a simultaneous proton transfer and C–C bond cleavage was also considered, using a smaller active site model consisting of 189 atoms. However, no such TS could be optimized. Every attempt to locate a concerted TS resulted in a stepwise mechanism.
- (33) Sheng, X.; Himo, F. *ACS Catal.* 2017, 7, 1733–1741.
- (34) Tsang, W. Y.; Wood, B. M.; Wong, F. M.; Wu, W.; Gerlt, J. A.; Amyes, T. L.; Richard, J. P. *J. Am. Chem. Soc.* 2012, 134, 14580–14594.
- (35) Vardi-Kilshtain, A.; Doron, D.; Major, D. T. *Biochemistry* 2013, 52, 4382–4390.